

Biochemical Studies of a Cyanobacterial Halogenase Support the Involvement of a Dimetal Cofactor

Published as part of *Biochemistry* special issue “A Tribute to Christopher T. Walsh”.

Michelle L. Wang, Nathaniel R. Glasser, Mrutyunjay A. Nair, Carsten Krebs,* J. Martin Bollinger, Jr.,* and Emily P. Balskus*



Cite This: *Biochemistry* 2025, 64, 2173–2180



Read Online

ACCESS |



Metrics & More



Article Recommendations



Supporting Information

ABSTRACT: Halogenation is a prominent transformation in natural product biosynthesis, with over 5000 halogenated natural products known to date. Biosynthetic pathways accomplish the synthetic challenge of selective halogenation, especially at unactivated sp^3 carbon centers, using halogenase enzymes. The halogenase CylC, discovered as part of the cylindrocyclophane (*cyl*) biosynthetic pathway, performs a highly selective chlorination reaction on an unactivated sp^3 carbon center and is proposed to use a dimetal cofactor. Putative dimetal halogenases are widely distributed across cyanobacterial biosynthetic pathways. However, rigorous *in vitro* biochemical and structural characterization of these enzymes has been challenging. Here, we report additional bioinformatic analyses of putative dimetal halogenases and the biochemical characterization of a newly identified CylC homologue. Site-directed mutagenesis identifies highly conserved putative metal-binding residues, and Mössbauer spectroscopy provides direct evidence for the presence of a diiron cofactor in these halogenases. These insights suggest mechanistic parallels between diiron and mononuclear nonheme iron halogenases, with the potential to guide further characterization and engineering of this unique subfamily of metalloenzymes.

Microbial natural product biosynthesis uses a broad range of enzymatic transformations to generate structurally complex, bioactive products.¹ One of the most striking and versatile microbial biosynthetic transformations is halogenation. Halogenation is widespread across all domains of life, with over 5000 halogenated natural products identified.² This modification alters the physiochemical properties and bioactivity of molecules, with approximately 25% of all drugs and drug candidates containing a C–X (where X = F, Cl, Br, or I) bond.³ While synthetic chemists face significant challenges in selective halogenation,⁴ Nature has evolved halogenases, enzymes that perform this chemistry with remarkable efficiency and selectivity.

All well-characterized halogenases belong to one of three major classes: electrophilic (C–X bond formed by nucleophilic attack on an electrophilic RO–X species), radical nonheme mononuclear iron (C–X bond formed by selective radical transfer), and SAM-dependent nucleophilic (C–X bond formed by S_N2 substitution).⁵ There has been significant interest in the characterization and discovery of enzymes that halogenate unactivated C(sp^3)–H bonds. For many years this type of reactivity was thought to be unique to nonheme mononuclear iron halogenases, which utilize oxygen, α -ketoglutarate, and a mononuclear iron cofactor to form the C–X bond (where X = Cl or Br) (Figure 1A). SyrB2, reported by Walsh and co-workers in 2005,⁶ was the first example of enzymatic oxidative halogenation in nonheme iron enzymes, enabling the discovery of many related enzymes.^{7–9} The crystal structure of SyrB2, solved by Drennan and Walsh, contained a 2 His–Cl facial triad, with the chloride replacing the

carboxylate ligand of the Asp residue found in analogous hydroxylases.¹⁰ This structural insight highlighted the possibility of a mechanism involving the iron-bound chloride. Indeed, subsequent mechanistic studies of these halogenases determined that reactive ferryl–oxo intermediates selectively abstract hydrogen atoms from unactivated C(sp^3) centers and C–X bonds are formed by a highly selective radical rebound with the halide ligated to the iron center.^{7,10–12} These fundamental studies have informed engineering of radical halogenases, expanding substrate scope to include non-natural, free-standing substrates and altering reactivity to enable bromination and azidation.^{13,14}

In 2017, we discovered a new radical halogenating enzyme in the biosynthesis of cylindrocyclophane F by the Cyanobacterium *Cylindrospermum lichenforme* (Figure 1B).¹⁵ Encoded within the *cyl* biosynthetic gene cluster (BGC), CylC performs a highly regio- and stereoselective chlorination at C₆ of its acyl carrier protein (ACP)-tethered substrate, CylB-decanoyl thioester. The resulting R-configured alkyl chloride is further elaborated to a chlorinated alkyl resorcinol intermediate, which undergoes a C–C bond forming dimerization by the Friedel–Crafts alkylating enzyme CylK to form the

Received: October 25, 2024

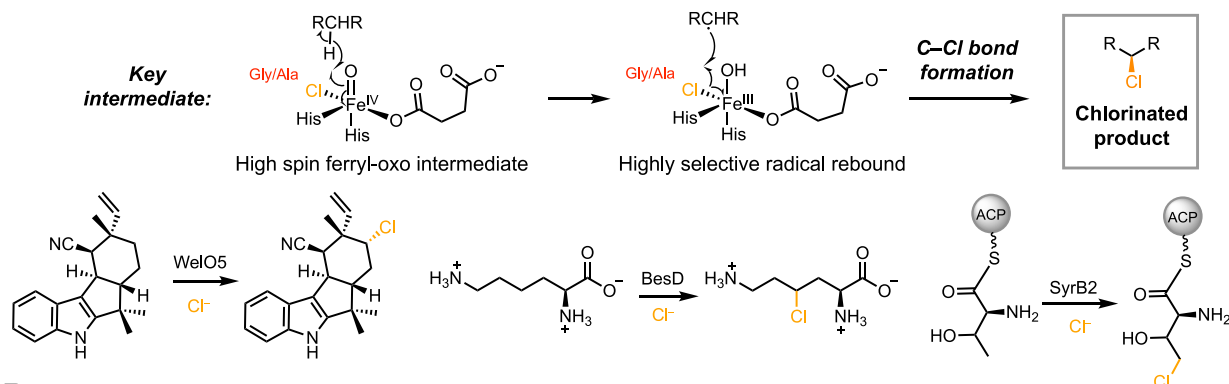
Revised: April 8, 2025

Accepted: April 10, 2025

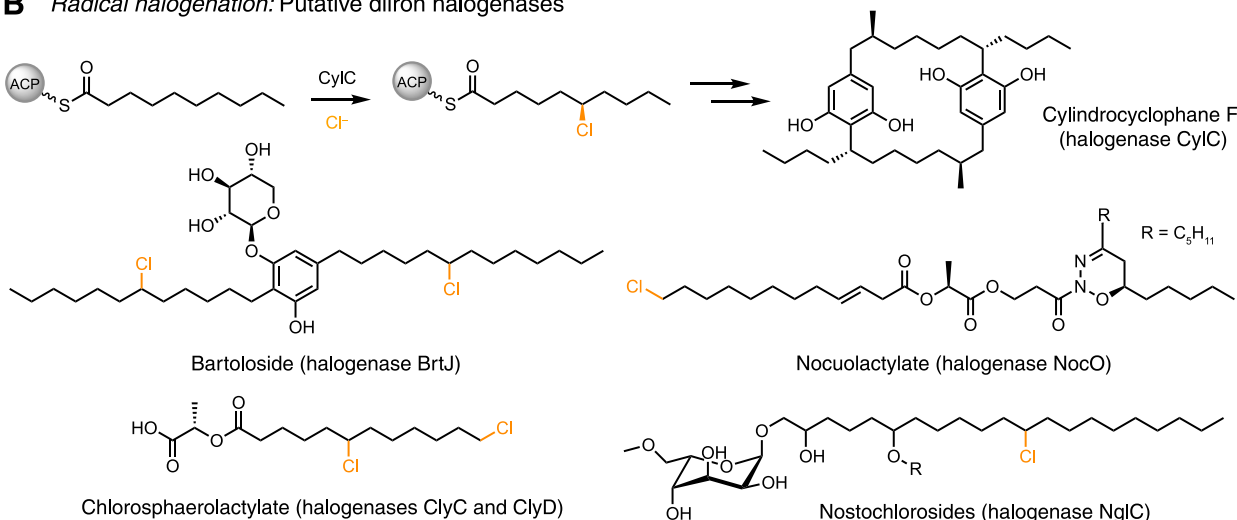
Published: April 29, 2025



A Radical halogenation: Nonheme mononuclear iron, α -KG dependent halogenases



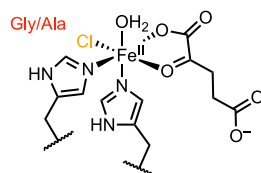
B Radical halogenation: Putative diiron halogenases



C

Previously reported:
Nonheme mononuclear
iron halogenases

- mononuclear nonheme iron center
- carboxylate ligand replaced by halide



This work:
Nonheme diiron
halogenases

Diiron cofactor detected via
Mössbauer spectroscopy

- proposed FDO-like diiron binding site
- carboxylate ligand replaced by halide

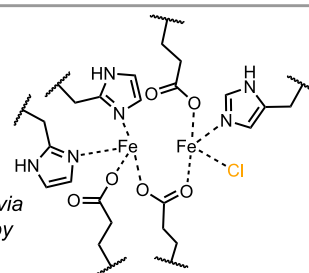


Figure 1. Radical halogenases functionalize unactivated carbon centers. (A) Overall reaction and examples of radical halogenation by mononuclear nonheme iron halogenases. (B) Putative diiron halogenases biosynthesize fatty acid-derived cyanobacterial natural products. (C) Characterization of active site residues and spectroscopy suggest putative diiron halogenases use a diiron cofactor for radical halogenation.

paracyclophane scaffold.^{15,16} Initial bioinformatic analyses revealed that CylC does not share any amino acid sequence similarity with known radical halogenases. While its halogenation activity was iron-dependent, it did not require cofactors or cosubstrates associated with enzymatic halogenation (heme, flavin, vanadate, α -ketoglutarate, *S*-adenosyl methionine). Instead, CylC resembles the ferritin-like diiron oxygenase AurF, which performs a 6-electron *N*-oxidation of *p*-amino-benzoic acid to *p*-nitrobenzoic acid in aureothin biosynthesis.¹⁷ Despite low amino acid similarity (26%) and identity (12%) between the two enzymes, aligning an initial homology model of CylC with AurF's crystal structure identified a set of putative CylC metal binding residues in the location of AurF's diiron

metallocofactor, leading to the hypothesis that CylC also possesses a dimetal cofactor. Initial biochemical experiments provided support for the hypothesis that CylC is a diiron enzyme by revealing an iron:enzyme ratio of $\sim 2:1$.¹⁵

Ferritin-like diiron oxygenases and oxidases (FDOs) are nonheme diiron enzymes that perform a wide variety of chemical reactions by activating molecular oxygen, inducing a transition from a typical diferrous resting state to a diferric state.^{18,19} Conversion of the corresponding diiron- O_2 adduct to various reactive intermediates enables oxidative transformations including *N*-oxygenation,¹⁷ alkane hydroxylation,²⁰ site-selective desaturation,²¹ and alkene epoxidation.²² Despite this broad reaction scope, diiron enzymes are not known to

perform halogenation, potentially making CylC the founding member of a new FDO subfamily.

Subsequent studies of putative diiron halogenases have largely focused on their genomic distribution and their associations with natural products. A survey of genomes and a PCR screen of cyanobacterial isolates revealed that CylC homologues are widespread across all major cyanobacterial classes, making them a major C–H functionalization strategy in the phylum. They are encoded within BGCs that are predicted to give rise to diverse molecular architectures²³ and participate in the biosyntheses of additional chlorinated fatty acid-derived natural products and biosynthetic intermediates (Figure 1B).^{24–28}

Despite the prevalence of putative diiron halogenases, little is known about the biochemical and structural basis for their halogenation activity. Beyond the previous preliminary studies of CylC, no reports have characterized the metallocofactor or key catalytic or metal binding residues of these enzymes. Notably, *in vitro* biochemical and structural experiments using these enzymes have been hindered by their general intractability and insolubility: initial studies of CylC required two coexpression partners, the fatty acid activating ligase (FAAL) CylA and the ACP CylB, to obtain low levels of soluble enzyme from an *Escherichia coli* expression system. Given that putative diiron halogenases represent a major C–H functionalization strategy in cyanobacteria, gaining a more detailed understanding of their structures and mechanisms would provide valuable insights into a chemically important biosynthetic transformation and new mode of reactivity for the nonheme diiron cofactor.

Here, we use bioinformatic, biochemical, and spectroscopic approaches to identify a proposed mode of diiron binding among dimetal halogenases. Multiple sequence alignments and structural predictions of CylC homologues reveal a highly conserved putative diiron binding site that may contain an open site for chloride binding. Using site-directed mutagenesis of the CylC homologue NocO, we show these proposed active site residues likely contribute to metal binding and chlorination activity. The lack of activity in these variants suggests the relevance of these residues in metallocofactor assembly. Finally, we use Mössbauer spectroscopy to obtain direct evidence of a diiron cofactor in NocO. Together, this work provides experimental support for the involvement of a diiron metallocofactor in this subfamily of radical halogenases (Figure 1C).

To guide further biochemical studies of putative diiron halogenases, we aligned the amino acid sequences of CylC, selected homologues, and the diiron *N*-oxygenase AurF (Figure 2A, Figure S1). This analysis identified candidate active site residues in the diiron halogenases based on the previously established iron binding ligands in AurF.²⁹ We located nine residues, seven of which are found in a QExxH and HxxDExxH motif, that most likely comprise the active site in the selected homologues. A further examination of 241 other CylC homologues identified in a BLAST search revealed that these nine residues are conserved in the dimetal halogenase subfamily (Figure 2A, Figure S2). We used both AlphaFold2 and AlphaFold3 to generate predicted structures of CylC and superimposed them onto the crystal structure of diiron-bound AurF to identify roles for these residues. Consistent with the prior homology model, CylC is predicted to have the distinctive four α -helix bundle characteristic of FDOs, with a glutamate- and histidine-rich active site (Figure

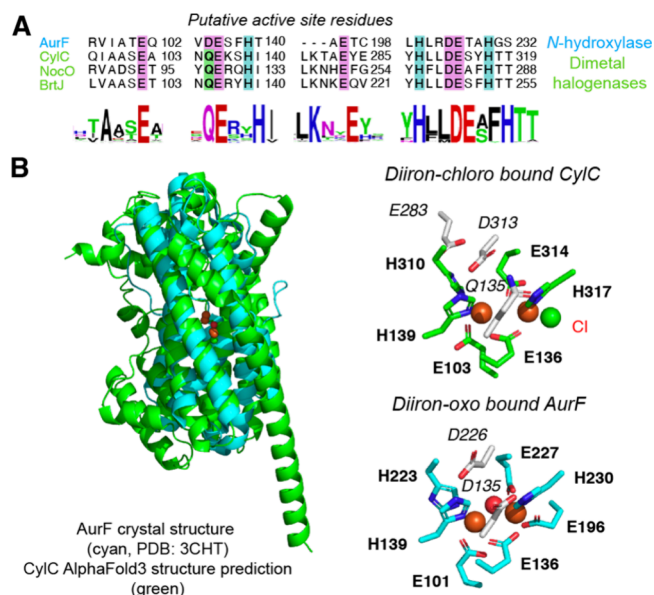


Figure 2. Bioinformatic analyses of CylC homologues predict amino acids involved in dimetal cofactor binding and identify a potential chloride binding site. (A) Protein sequence alignment of AurF with select CylC homologues reveals a set of putative active site residues. (B) AlphaFold3 predicted structure of CylC contains the FDO-like fold found in AurF and a dimetallocofactor with an open coordination site for halide binding. Italicized residues represent active site residues that are predicted to not directly participate in metal binding.

2B, Figures S3, S4).^{18,30} The AlphaFold structures predicted roles in metal binding and hydrogen bonding for the nine residues we had identified in our sequence alignment. In AurF's crystal structure, two aspartates (D135 and D226) act as bases and hydrogen bond acceptors for H230 and H139, respectively, allowing the two histidine residues to be stronger ligands for the diiron cofactor.²⁹ In CylC and its homologues, D135 is replaced by a glutamine, which lacks the basicity of an aspartate residue, potentially altering the metal binding environment in dimetal halogenases. However, there are differences in the predicted metal binding ligands. The 3 histidine/4 carboxylate diiron binding mode of AurF is largely unique to the *N*-oxygenase subfamily of FDOs, with most other FDOs having a six-coordinate iron-binding environment. Specifically, most nonheme diiron hydroxylases bind the diiron cofactor using a 2 histidine/4 carboxylate motif.³¹ The AlphaFold structure predicts that CylC has six primary metal binding ligands as compared to AurF's seven. However, in contrast to other C–H oxidizing FDOs, the metal binding environment of CylC is predicted to contain a 3 histidine/3 glutamate motif resembling AurF's active site. Notably, the final coordination site in the predicted structures of CylC and other homologues, occupied by E196 in AurF and E283 in the original CylC homology model, is predicted to be left unoccupied by a shift of this glutamate to outside the primary metal binding sphere (Figures S4, S7). Docking two iron atoms and a chloride ion with AlphaFold3 suggested that this predicted open coordination site could accommodate a chloride ion, a structural feature reminiscent of the chloride binding site of nonheme mononuclear iron halogenases (Figure 2B).¹⁰ Inspecting the sequence alignment of CylC homologues revealed that this glutamate is the only residue among the nine identified that is not absolutely conserved; a small subset of sequences have glutamine at this position

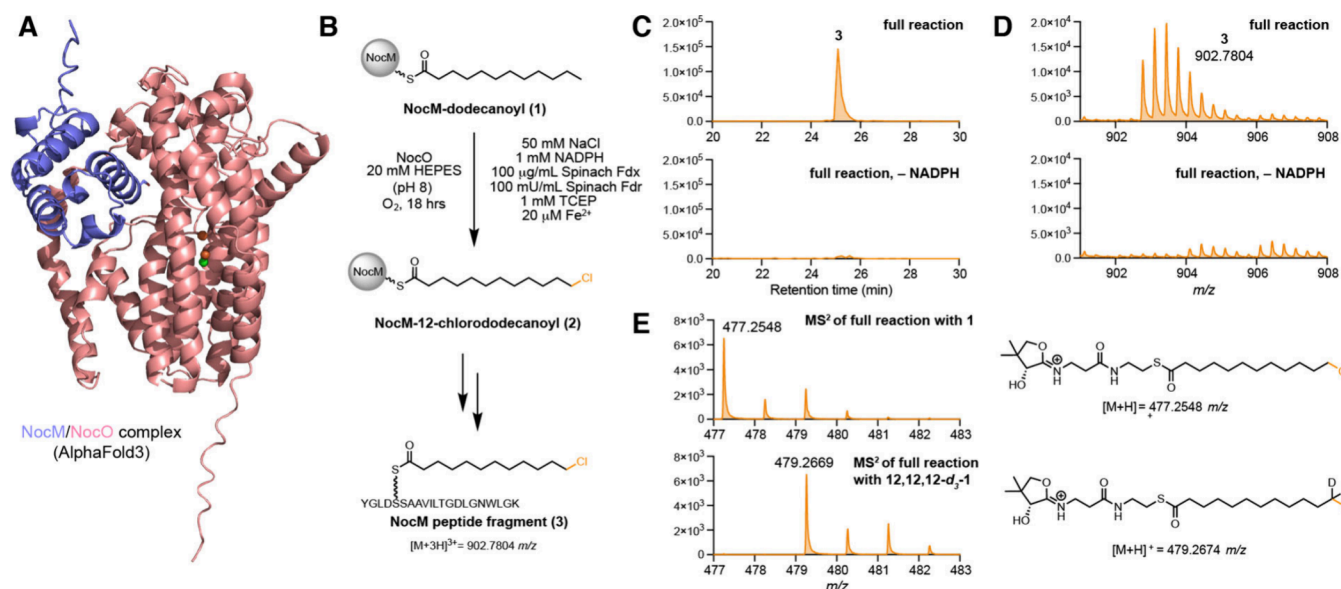


Figure 3. NocO chlorinates the terminal position of NocM-tethered dodecanoyl thioester. (A) AlphaFold3 predicted structure of the NocM/NocO complex. (B) *In vitro* assay for halogenation of 1 by NocO (Fdx = ferredoxin, Fdr = ferredoxin reductase). (C) Representative extracted ion chromatogram (EIC) of trypsin digested product 3 in full *in vitro* reactions and reactions lacking the electron source NADPH. (D) Representative MS spectra of 3 extracted from EICs in (C). (E) MS/MS fragmentation of product in reactions supplemented with NocL-loaded NocM-12,12,12-d₃-dodecanoyl thioester shows NocO selectively halogenates the terminal carbon of the acyl chain of 1. Assays and negative controls were performed in triplicate for experiments in (C) and (D), assays and negative controls were performed in duplicate for the isotopic labeling experiment in (E).

(Figure S2). A search of residues within 5 Å of the putative chloride-bound iron atom did not reveal any additional residues that could act as metal-binding ligands, further supporting the possibility of halide coordination at this site (Figures S7, S8). By predicting features distinct from AurF and the original CylC homology model, these analyses potentially redefine the active sites of putative dimetal halogenases.

To functionally characterize the putative active site residues in CylC homologues, we sought a more tractable enzyme for *in vitro* studies. As highlighted above, biochemical studies of CylC have been complicated by its poor solubility, instability, and strict need for two coexpression partners.¹⁵ Therefore, we screened 12 phylogenetically diverse CylC homologues²³ for improved solubility and expression in *E. coli* (Table S3). We attempted heterologous expression under a variety of conditions, including different host strains, temperatures, promoters, and coexpression with a cognate ACP. This screening effort identified one homologue, NocO (43% amino acid ID, 60% similarity), from *Nodulariasp.* LEGE 06071, with improved expression characteristics, namely its ability to be solubly expressed with just its cognate ACP, NocM (Figure 3A). We selected NocO as a model system to study dimetal halogenases.

NocO is encoded by the *noc* BGC which produces the nocuolactylates.²⁷ It is hypothesized to chlorinate an ACP-tethered dodecanoyl thioester starter unit (1) in the assembly of the chlorosphaerolactylate half of the nocuolactylates.^{26,27} We expressed and purified NocO together with its ACP, NocM, as *N*-terminally His₆-tagged constructs from *E. coli* BL21(DE3) (Figure S9). Since NocM was purified in its apo form, we used the phosphopantetheinyl transferase Sfp to generate 1 from dodecanoyl CoA (Figure 3B). We reconstituted NocO's chlorination activity toward 1 *in vitro* by combining the enzyme–substrate mixture with redox components required for CylC activity.¹⁶ Reactions supple-

mented with an exogenous ferrous source (Figure 3C, 3D) and reactions with the as-purified protein (Figure S14) all generated monochlorinated 2. When a terminally deuterated version of 1 was tested, a + 2 *m/z* shift was observed in the phosphopantetheine ejection fragment, confirming NocO's selectivity for the terminal position of its substrate (Figure 3E). We were unable to detect hydroxylated products in NocO assays, a known chemoselectivity issue in nonheme mononuclear iron halogenases.^{32–35} The reconstitution of NocO's chlorination activity confirmed its role as a halogenase.

We next set out to investigate the importance of the predicted metal binding residues in NocO. However, the previously established heterologous expression system failed to yield appreciable amounts of soluble mutant enzymes, which prevented biochemical experiments. Similar expression difficulties were reported for AurF upon mutation of its metal-binding active site residues.³⁶ We made several attempts to increase protein yield, including scaling up expression cultures, expressing a SUMO-tagged construct, and coexpression with both NocM and the FAAL NocL, without success. We next explored changing the heterologous expression host and discovered that *E. coli* ArcticExpress (DE3), a BL21 derivative that constitutively expresses the chaperones Cpn60 and Cpn10 from *Oleispira antarctica*, produced our variants at comparable levels to wild-type NocO when coexpressed with NocM (Figure S17). The two proteins also copurify with Cpn60 (Figure S18). Using this expression system, we reconstituted wild-type NocO's *in vitro* chlorination activity (Figure 4C). In addition, a Ferene-S assay revealed approximately 1.97 mol Fe/mol in wild-type NocO, which is consistent with a diiron cofactor. This observation, in combination with NocO's homology with CylC and its demonstrated halogenation activity, supports the assignment of NocO as a dimetal halogenase.

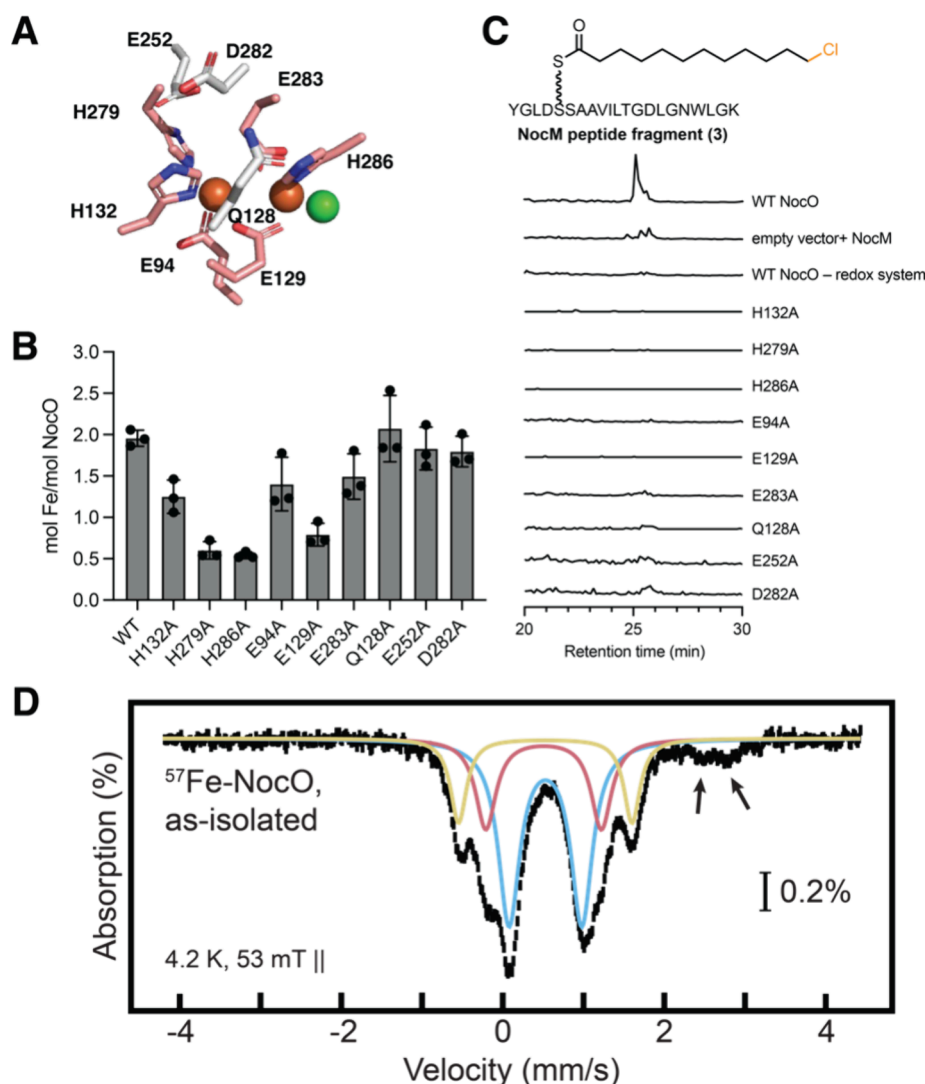


Figure 4. Mutation of predicted metal binding residues and Mössbauer spectroscopy support the presence of a diiron cofactor in NocO. (A) Putative active site residues in NocO identified in an AlphaFold3-predicted structure. Residues shown in white are predicted to be not directly involved in metal binding. (B) Representative EICs for 3 show that active site variants are catalytically inactive. (C) Certain active site variants show decreased iron loading relative to WT NocO. Assays and corresponding negative controls were performed in triplicate, bars represent mean \pm SD. (D) 4.2-K/53-mT Mössbauer spectrum of ^{57}Fe -enriched, aerobically isolated NocO. The experimental spectrum is depicted in black vertical bars of heights reflecting the standard deviations of the absorption values during spectral acquisition. The blue, red, and yellow lines are quadrupole doublet simulations illustrating the fractional contributions from the different diiron(III)-species quoted in the text. The black arrows represent the high-energy lines of the Fe(II)-species, as quoted in the text. The parameters of the different iron-species used for simulation are summarized in Table S7.

Substituting alanine in place of any of the nine putative active site residues revealed that all of them were essential for chlorination activity (Figure 4A,C). However, only the six variants that replace a proposed metal binding ligand showed reduced iron binding relative to wild-type, consistent with a near single occupancy-like state (Figure 4B). Interestingly, the Q128A, E252A, and D282A variants all had comparable iron stoichiometry relative to the wild-type enzyme. This finding supports the hypothesis that E252 is likely not a metal binding residue and instead suggests that D282 and E252 may act as hydrogen bond acceptors for their proximal iron-binding histidine residues and that their mutation to alanine may hinder catalytic activity without affecting metal acquisition. While these iron:protein stoichiometries are approximate due to the challenge of accurately quantifying NocO in our enzyme preparations, the absence of chlorination activity in these

variants is consistent with their proposed roles as first- and second-sphere cofactor ligands.

To directly investigate the nature of NocO's metal cofactor, we purified ^{57}Fe -enriched NocO on a large scale for Mössbauer spectroscopy. The UV/vis absorption spectrum of the as isolated sample exhibited broad absorbance features at ~ 360 nm and ~ 410 nm (Figure S11), of which the former is likely characteristic of an oxo-to-iron ligand-to-metal charge transfer band found in other members of the FDO family, typically indicative of a μ -oxo- $\text{Fe}_2^{\text{III/III}}$ species.³⁷ The 4.2-K/53-mT spectrum of the ^{57}Fe -enriched, aerobically isolated protein (Figure 4D, black vertical bars) can be simulated as three partially resolved quadrupole doublets with isomer shifts (δ) and quadrupole splitting (ΔE_Q) ($\delta_1 = 0.53$ mm/s, $\Delta E_{Q1} = 0.90$ mm/s, 50% of total absorption, blue line; $\delta_2 = 0.51$ mm/s, $\Delta E_{Q2} = 1.43$ mm/s, 23% of total absorption, red line; and $\delta_3 =$

0.53 mm/s, $\Delta E_Q = 2.15$ mm/s, 17% of total absorption, yellow line) characteristic of antiferromagnetically coupled high-spin diferric clusters with diamagnetic ($S = 0$) electron-spin ground states (Table S7).^{38,39} The unusually large quadrupole splitting of the species outlined in yellow suggests the presence of a μ -oxo-bridge,⁴⁰ as has been observed in other FDOs, such as the β subunit of class Ia ribonucleotide reductase from *Escherichia coli*^{41–43} and the *N*-oxygenase AurF.⁴⁴ In addition, there are two weak absorption features at ~ 2.5 and ~ 2.8 mm/s, positions typical for the high-energy lines of quadrupole doublets arising from high-spin Fe(II) ions (Figure 4D, black arrows). The spectrum of an equivalent sample reduced anoxically with excess sodium dithionite (Figure S12, black vertical bars) shows an increased intensity from these absorption features, which contribute $\sim 60\%$ of the total absorption area and have parameters ($\delta \sim 1.2$ mm/s, $\Delta E_Q \sim 3.0$ mm/s) typical of nitrogen and oxygen coordinated high-spin Fe(II) species.^{38,44,45} In the reduced sample, two minor absorption features (with $\sim 20\%$ of the total absorption area each) with their high-energy lines at positions ~ 1 and ~ 1.6 mm/s, (Figure S12, black arrows) show that the diferric species remain after reduction only by dithionite, suggesting the need for a mediator to access the buried cofactor. The Mössbauer data thus provide definitive evidence for the presence of a nonheme diiron cofactor in NocO.

In summary, these findings support the involvement of a diiron cofactor in a distinct group of radical halogenases. By combining information from multiple sequence alignments and predicted enzyme structures, we identified a conserved set of putative metal binding residues and a potential open coordination site for chloride binding in CylC and its homologues. In addition, the predicted 3 histidine/3 glutamate architecture is distinct from that of diiron alkane hydroxylases and *N*-oxygenases, the closest structurally characterized homologues of this halogenase family.^{29,46} The predicted change of the aspartate hydrogen bond acceptor in FDOs to a glutamine in dimetal halogenases may also have implications for chemoselectivity and mechanism. Further studies will be needed to determine the exact nature of the ligands bound to the diiron cofactor, but the conservation of these identified residues suggests that they are functionally important.

To overcome difficulties heterologously expressing CylC, we evaluated multiple homologues, ultimately identifying NocO as the most viable candidate for biochemical studies. NocO purified from *E. coli* catalyzes a highly chemo- and regioselective chlorination of the terminal carbon of an ACP-tethered dodecanoyl thioester. Mutagenesis of active site residues has been important for understanding mononuclear nonheme Fe-dependent halogenases,⁴⁷ but has been challenging in FDOs.³⁶ The mutagenesis of putative metal-binding residues in NocO suggests they are essential for chlorination activity and diiron metallocofactor assembly. Importantly, the Mössbauer spectrum of as-isolated NocO exhibits primarily quadrupole doublet features indicative of antiferromagnetically coupled diiron(III) clusters, providing the first direct spectroscopic evidence for the identity of the metallocofactor in this group of halogenases.

Our results provide exciting insights into the potential mechanism and evolution of these enzymes. The high bond dissociation energies of $C(sp^3)$ –H bonds (~ 98 – 101 kcal/mol)⁴⁸ and the unactivated nature of the carbon centers functionalized by diiron halogenases necessitates a radical-based halogenation mechanism.² The enzymatic halogenation

of $C(sp^3)$ –H bonds has been of longstanding interest to both biological and synthetic chemists. From the initial characterization of the mononuclear Fe-dependent radical halogenases¹¹ to recent reports of a dicopper radical halogenase,⁴⁹ these halogenases are proposed to share certain mechanistic features. In mononuclear Fe-dependent radical halogenases, the carboxylate ligand found in related hydroxylases is mutated to a smaller, nonpolar residue to allow the binding of a halide to iron, and the C–X bond is formed through a radical rebound following the activation of the iron cofactor by molecular oxygen.¹⁰ Similarly, the proposed mechanism of the recently discovered dicopper halogenase ApnU also invokes hydrogen atom abstraction by an O_2 -activated metallocofactor followed by a radical transfer of a directly coordinated halogen.⁴⁹ We propose the involvement of an analogous diiron–chloro metallocofactor in the diiron halogenases and a mechanistic hypothesis involving C–H abstraction by a high-spin diiron–oxo species (Figure S21). Many aspects of this mechanistic hypothesis, specifically the formation of a di-Fe(IV) intermediate, are similar to intermediate Q in soluble methane monooxygenase (sMMO).^{20,50} However, we propose that chlorination occurs via a chlorine transfer step resembling that of the mononuclear iron halogenases (Figure S21). This proposal could account for the reactivity of diiron halogenases. Moreover, this mechanism suggests that like the mononuclear nonheme radical halogenases, diiron halogenases may have evolved from hydroxylating diiron enzymes. This parallel evolution in biochemical logic may inform efforts to engineer halogenase activity in diiron hydroxylase enzymes, which has been explored in their mononuclear iron counterparts.^{32,34,51} Efforts to structurally characterize NocO and study the mechanism of diiron-catalyzed chlorination are ongoing. Additional insights into this halogenase family will continue to broaden our knowledge of enzymatic C–H functionalization in natural product biosynthesis.

■ ASSOCIATED CONTENT

Supporting Information

The Supporting Information is available free of charge at <https://pubs.acs.org/doi/10.1021/acs.biochem.4c00720>.

Experimental details, primers used for plasmid construction, and supplemental LC/MS data (PDF)

Accession Codes

The following are the NCBI Accession Codes for the enzymes characterized in this study: NocL (QOV09198.1), NocM (QOV09191.1), and NocO (QOV09192.1). The following are the UniProt identifiers for the enzymes characterized in this study: NocL (A0A7S6RCM7), NocM (A0A7U3NLF1), and NocO (A0A7U3NLB0).

■ AUTHOR INFORMATION

Corresponding Authors

Emily P. Balskus – Department of Chemistry and Chemical Biology, Harvard University, Cambridge, Massachusetts 02138, United States; Howard Hughes Medical Institute, Harvard University, Cambridge, Massachusetts 02138, United States; orcid.org/0000-0001-5985-5714; Email: balskus@chemistry.harvard.edu

Carsten Krebs – Department of Chemistry, The Pennsylvania State University, University Park, Pennsylvania 16802, United States; Department of Biochemistry and Molecular Biology, The Pennsylvania State University, University Park,

Pennsylvania 16802, United States; orcid.org/0000-0002-3302-7053; Email: ckrebs@psu.edu

J. Martin Bollinger, Jr. – Department of Chemistry, The Pennsylvania State University, University Park, Pennsylvania 16802, United States; orcid.org/0000-0003-0751-8585; Email: jmb21@psu.edu

Authors

Michelle L. Wang – Department of Chemistry and Chemical Biology, Harvard University, Cambridge, Massachusetts 02138, United States; orcid.org/0000-0001-9836-3798

Nathaniel R. Glasser – Department of Chemistry and Chemical Biology, Harvard University, Cambridge, Massachusetts 02138, United States

Mrutyunjay A. Nair – Department of Chemistry, The Pennsylvania State University, University Park, Pennsylvania 16802, United States

Complete contact information is available at:

<https://pubs.acs.org/10.1021/acs.biochem.4c00720>

Author Contributions

M.L.W., N.R.G., and M.A.N. designed and conducted the experiments in this work and analyzed the data. All authors wrote the manuscript. All authors have given approval of the final version of the manuscript.

Funding

This work was supported by grants from the National Science Foundation (CHE-2003436) and the National Institutes of Health (SR01GM132564) to E.P.B. E.P.B. is an HHMI investigator. N.R.G. was supported by an NSF Postdoctoral Research Fellowship in Biology under grant no. 1907240. C.K. is supported by a MIRA grant from the National Institutes of Health (SR35GM127079).

Notes

The authors declare no competing financial interest.

ACKNOWLEDGMENTS

The authors acknowledge Samantha Cassell for initial efforts to screen halogenases for improved expression and Ronak Desai for his help in mutant expression screening. The authors would like to thank Dr. Nathaniel Braffman, Dr. Anne Marie Crooke, Dr. Grace Kenney, Dr. Gil Namkoong, Dr. Antonio Tinoco Valencia, and Dr. Beverly Fu for their insight and helpful discussions on experimental details. The authors also acknowledge Dr. Jake Essman for providing feedback on the manuscript. We note that this article is subject to HHMI's Open Access to Publications policy. HHMI laboratory heads have previously granted a nonexclusive CC BY 4.0 license to the public and a sublicensable license to HHMI in their research articles. Pursuant to those licenses, the author-accepted manuscript of this article can be made freely available under a CC BY 4.0 license immediately upon publication.

DEDICATION

This contribution is dedicated to the memory of Professor Christopher T. Walsh, an important mentor to E.P.B. and J.M.B., whose foundational work on halogenases in natural product biosynthesis inspired this study.

ABBREVIATIONS

EIC, extracted ion chromatogram; LC/MS, liquid chromatography/mass spectrometry; MS, mass spectrometry; NADPH, nicotinamide adenine dinucleotide phosphate.

REFERENCES

- (1) Pham, J. V.; Yilma, M. A.; Feliz, A.; Majid, M. T.; Maffetone, N.; Walker, J. R.; Kim, E.; Cho, H. J.; Reynolds, J. M.; Song, M. C.; Park, S. R.; Yoon, Y. J. A Review of the Microbial Production of Bioactive Natural Products and Biologics. *Frontiers in Microbiology* **2019**, *10*, 1.
- (2) Fraley, A. E.; Sherman, D. H. Halogenase Engineering and Its Utility in Medicinal Chemistry. *Bioorg. Med. Chem. Lett.* **2018**, *28* (11), 1992–1999.
- (3) Wishart, D. S.; Feunang, Y. D.; Guo, A. C.; Lo, E. J.; Marcu, A.; Grant, J. R.; Sajed, T.; Johnson, D.; Li, C.; Sayeeda, Z.; Assempour, N.; Iynkkaran, I.; Liu, Y.; Maciejewski, A.; Gale, N.; Wilson, A.; Chin, L.; Cummings, R.; Le, D.; Pon, A.; Knox, C.; Wilson, M. DrugBank 5.0: A Major Update to the DrugBank Database for 2018. *Nucleic Acids Res.* **2018**, *46*, D1074–D1082.
- (4) Arndtsen, B. A.; Bergman, R. G.; Mobley, T. A.; Peterson, T. H. Selective Intermolecular Carbon–Hydrogen Bond Activation by Synthetic Metal Complexes in Homogeneous Solution. *Acc. Chem. Res.* **1995**, *28* (3), 154–162.
- (5) Crowe, C.; Molyneux, S.; Sharma, S. V.; Zhang, Y.; Gkotsi, D. S.; Connaris, H.; Goss, R. J. M. Halogenases: A Palette of Emerging Opportunities for Synthetic Biology–Synthetic Chemistry and C–H Functionalisation. *Chem. Soc. Rev.* **2021**, *50* (17), 9443–9481.
- (6) Vaillancourt, F. H.; Yin, J.; Walsh, C. T. SyrB2 in Syringomycin E Biosynthesis Is a Nonheme Fe(II) α -Ketoglutarate- and O₂-Dependent Halogenase. *Proc. Natl. Acad. Sci. U.S.A.* **2005**, *102* (29), 10111.
- (7) Galonić, D. P.; Vaillancourt, F. H.; Walsh, C. T. Halogenation of Unactivated Carbon Centers in Natural Product Biosynthesis: Trichlorination of Leucine during Barbamide Biosynthesis. *J. Am. Chem. Soc.* **2006**, *128* (12), 3900–3901.
- (8) Chang, Z.; Platt, P.; Gerwick, W. H.; Nguyen, V.-A.; Willis, C. L.; Sherman, D. H. The Barbamide Biosynthetic Gene Cluster: A Novel Marine Cyanobacterial System of Mixed Polyketide Synthase (PKS)-Non-Ribosomal Peptide Synthetase (NRPS) Origin Involving an Unusual Trichloroleucyl Starter Unit. *Gene* **2002**, *296* (1), 235–247.
- (9) Vaillancourt, F. H.; Yeh, E.; Vosburg, D. A.; O'Connor, S. E.; Walsh, C. T. Cryptic Chlorination by a Non-Haem Iron Enzyme during Cyclopropyl Amino Acid Biosynthesis. *Nature* **2005**, *436* (7054), 1191–1194.
- (10) Blasiak, L. C.; Vaillancourt, F. H.; Walsh, C. T.; Drennan, C. L. Crystal Structure of the Non-Haem Iron Halogenase SyrB2 in Syringomycin Biosynthesis. *Nature* **2006**, *440* (7082), 368–371.
- (11) Galonić, D. P.; Barr, E. W.; Walsh, C. T.; Bollinger, J. M., Jr.; Krebs, C. Two Interconverting Fe(IV) Intermediates in Aliphatic Chlorination by the Halogenase CytC3. *Nat. Chem. Biol.* **2007**, *3* (2), 113–116.
- (12) Matthews, M. L.; Krest, C. M.; Barr, E. W.; Vaillancourt, F. H.; Walsh, C. T.; Green, M. T.; Krebs, C.; Bollinger, J. M., Jr. Substrate-Triggered Formation and Remarkable Stability of the C–H-Cleaving Chloroferryl Intermediate in the Aliphatic Halogenase, SyrB2. *Biochemistry* **2009**, *48* (20), 4331–4343.
- (13) Matthews, M. L.; Chang, W.; Layne, A. P.; Miles, L. A.; Krebs, C.; Bollinger, J. M., Jr. Direct Nitration and Azidation of Aliphatic Carbons by an Iron-Dependent Halogenase. *Nat. Chem. Biol.* **2014**, *10* (3), 209–215.
- (14) Neugebauer, M. E.; Sumida, K. H.; Pelton, J. G.; McMurphy, J. L.; Marchand, J. A.; Chang, M. C. Y. A Family of Radical Halogenases for the Engineering of Amino-Acid-Based Products. *Nat. Chem. Biol.* **2019**, *15* (10), 1009–1016.
- (15) Nakamura, H.; Schultz, E. E.; Balskus, E. P. A New Strategy for Aromatic Ring Alkylation in Cylindrocyclophane Biosynthesis. *Nat. Chem. Biol.* **2017**, *13* (8), 916–921.

- (16) Nakamura, H.; Hamer, H. A.; Sirasani, G.; Balskus, E. P. Cyliindrocyclophane Biosynthesis Involves Functionalization of an Unactivated Carbon Center. *J. Am. Chem. Soc.* **2012**, *134* (45), 18518–18521.
- (17) Chanco, E.; Choi, Y. S.; Sun, N.; Vu, M.; Zhao, H. Characterization of the *N*-Oxygenase AurF from *Streptomyces thioletus*. *Bioorg. Med. Chem.* **2014**, *22* (20), 5569–5577.
- (18) Jasiewicz, A. J.; Que, L., Jr. Dioxygen Activation by Nonheme Diiron Enzymes: Diverse Dioxygen Adducts, High-Valent Intermediates, and Related Model Complexes. *Chem. Rev.* **2018**, *118* (5), 2554–2592.
- (19) Rajakovich, L. J.; Zhang, B.; McBride, M. J.; Boal, A. K.; Krebs, C.; Bollinger, J. M., Jr. S10 - Emerging Structural and Functional Diversity in Proteins With Dioxygen-Reactive Dinuclear Transition Metal Cofactors. In *Comprehensive Natural Products III*; Liu, H.-W. B., Begley, T. P., Eds.; Elsevier: 2020; pp 215–250.
- (20) Banerjee, R.; Proshlyakov, Y.; Lipscomb, J. D.; Proshlyakov, D. A. Structure of the Key Species in the Enzymatic Oxidation of Methane to Methanol. *Nature* **2015**, *518* (7539), 431–434.
- (21) Fox, B. G.; Lyle, K. S.; Rogge, C. E. Reactions of the Diiron Enzyme Stearoyl-Acyl Carrier Protein Desaturase. *Acc. Chem. Res.* **2004**, *37* (7), 421–429.
- (22) Small, F. J.; Ensign, S. A. Alkene Monooxygenase from *Xanthobacter* Strain Py2. *J. Biol. Chem.* **1997**, *272* (40), 24913–24920.
- (23) Eusebio, N.; Rego, A.; Glasser, N. R.; Castelo-Branco, R.; Balskus, E. P.; Leão, P. N. Distribution and Diversity of Dimetal-Carboxylate Halogenases in Cyanobacteria. *BMC Genomics* **2021**, *22* (1), 633.
- (24) Reis, J. P. A.; Figueiredo, S. A. C.; Sousa, M. L.; Leão, P. N. BrtB Is an O-Alkylating Enzyme That Generates Fatty Acid-Bartolose Esters. *Nat. Commun.* **2020**, *11* (1), 1458.
- (25) Lopez, J. A. V.; Petitbois, J. G.; Vairappan, C. S.; Umezawa, T.; Matsuda, F.; Okino, T. Columbamides D and E: Chlorinated Fatty Acid Amides from the Marine Cyanobacterium *Moorea bouillonii* Collected in Malaysia. *Org. Lett.* **2017**, *19* (16), 4231–4234.
- (26) Gutiérrez-del-Río, I.; Brugerolle de Fraissinette, N.; Castelo-Branco, R.; Oliveira, F.; Morais, J.; Redondo-Blanco, S.; Villar, C. J.; Iglesias, M. J.; Soengas, R.; Cepas, V.; Cubillos, Y. L.; Sampietro, G.; Rodolfi, L.; Lombó, F.; González, S. M. S.; López Ortiz, F.; Vasconcelos, V.; Reis, M. A. Chlorosphaerolactylates A–D: Natural Lactylates of Chlorinated Fatty Acids Isolated from the Cyanobacterium *Sphaerospermopsis* sp. LEGE 00249. *J. Nat. Prod.* **2020**, *83* (6), 1885–1890.
- (27) Martins, T. P.; Glasser, N. R.; Kountz, D. J.; Oliveira, P.; Balskus, E. P.; Leão, P. N. Biosynthesis of the Unusual Carbon Skeleton of Nocoulin A. *ACS Chem. Biol.* **2022**, *17*, 2528.
- (28) Glasser, N. R.; Cui, D.; Risser, D. D.; Okafor, C. D.; Balskus, E. P. Accelerating the Discovery of Alkyl Halide-Derived Natural Products Using Halide Depletion. *Nat. Chem.* **2024**, *16* (2), 173–182.
- (29) Choi, Y. S.; Zhang, H.; Brunzelle, J. S.; Nair, S. K.; Zhao, H. In Vitro Reconstitution and Crystal Structure of P-Aminobenzoate *N*-Oxygenase (AurF) Involved in Aureothin Biosynthesis. *Proc. Natl. Acad. Sci. U. S. A.* **2008**, *105* (19), 6858–6863.
- (30) Tosha, T.; Hasan, M. R.; Theil, E. C. The Ferritin Fe₂ Site at the Diiron Catalytic Center Controls the Reaction with O₂ in the Rapid Mineralization Pathway. *Proc. Natl. Acad. Sci. U.S.A.* **2008**, *105* (47), 18182–18187.
- (31) Kurtz, D. M. Structural Similarity and Functional Diversity in Diiron–Oxo Proteins. *JBIC* **1997**, *2* (2), 159–167.
- (32) Neugebauer, M. E.; Kissman, E. N.; Marchand, J. A.; Pelton, J. G.; Sambold, N. A.; Millar, D. C.; Chang, M. C. Y. Reaction Pathway Engineering Converts a Radical Hydroxylase into a Halogenase. *Nat. Chem. Biol.* **2022**, *18* (2), 171–179.
- (33) Mitchell, A. J.; Zhu, Q.; Maggiolo, A. O.; Ananth, N. R.; Hillwig, M. L.; Liu, X.; Boal, A. K. Structural Basis for Halogenation by Iron- and 2-Oxo-Glutamate-Dependent Enzyme WelO5. *Nat. Chem. Biol.* **2016**, *12* (8), 636–640.
- (34) Mitchell, A. J.; Dunham, N. P.; Bergman, J. A.; Wang, B.; Zhu, Q.; Chang, W.; Liu, X.; Boal, A. K. Structure-Guided Reprogramming of a Hydroxylase To Halogenate Its Small Molecule Substrate. *Biochemistry* **2017**, *56* (3), 441–444.
- (35) Matthews, M. L.; Neumann, C. S.; Miles, L. A.; Grove, T. L.; Booker, S. J.; Krebs, C.; Walsh, C. T.; Bollinger, J. M., Jr. Substrate Positioning Controls the Partition between Halogenation and Hydroxylation in the Aliphatic Halogenase, SyrB2. *Proc. Natl. Acad. Sci. U. S. A.* **2009**, *106* (42), 17723–17728.
- (36) Simurdiak, M.; Lee, J.; Zhao, H. A New Class of Arylamine Oxygenases: Evidence That p-Aminobenzoate *N*-Oxygenase (AurF) Is a Di-Iron Enzyme and Further Mechanistic Studies. *ChemBioChem* **2006**, *7* (8), 1169–1172.
- (37) Brown, C. A.; Remar, G. J.; Musselman, R. L.; Solomon, E. I. Spectroscopic and Electronic Structure Studies of Met-Hemerythrin Model Complexes: A Description of the Ferric–Oxo Dimer Bond. *Inorg. Chem.* **1995**, *34* (3), 688–717.
- (38) Münck, E. In *Physical Methods in Bioinorganic Chemistry*; University Science Books: 2000; p 287.
- (39) Gütllich, P.; Bill, E.; Trautwein, A. X. *Mössbauer Spectroscopy and Transition Metal Chemistry: Fundamentals and Applications*; Springer Berlin Heidelberg: 2011.
- (40) Vincent, J. B.; Olivier-Lilley, G. L.; Averill, B. A. Proteins Containing Oxo-Bridged Dinuclear Iron Centers: A Bioinorganic Perspective. *Chem. Rev.* **1990**, *90* (8), 1447–1467.
- (41) Atkin, C. L.; Thelander, L.; Reichard, P.; Lang, G. Iron and Free Radical in Ribonucleotide Reductase: Exchange of iron and Mössbauer spectroscopy of the protein B2 Subunit of the *Escherichia coli* enzyme. *J. Biol. Chem.* **1973**, *248* (21), 7464–7472.
- (42) Lynch, J. B.; Juarez-Garcia, C.; Münck, E.; Que, L., Jr. Mössbauer and EPR Studies of the Binuclear Iron Center in Ribonucleotide Reductase from *Escherichia coli*. *J. Biol. Chem.* **1989**, *264* (14), 8091–8096.
- (43) Wörsdörfer, B.; Conner, D. A.; Yokoyama, K.; Livada, J.; Seyedsayamdost, M.; Jiang, W.; Silakov, A.; Stubbe, J.; Bollinger, J. M., Jr.; Krebs, C. Function of the Diiron Cluster of *Escherichia coli* Class Ia Ribonucleotide Reductase in Proton-Coupled Electron Transfer. *J. Am. Chem. Soc.* **2013**, *135* (23), 8585–8593.
- (44) Korboukh, V. K.; Li, N.; Barr, E. W.; Bollinger, J. M., Jr.; Krebs, C. A Long-Lived, Substrate-Hydroxylating Peroxodiiron(III/III) Intermediate in the Amine Oxygenase, AurF, from *Streptomyces thioleus*. *J. Am. Chem. Soc.* **2009**, *131* (38), 13608–13609.
- (45) Makris, T. M.; Vu, V. V.; Meier, K. K.; Komor, A. J.; Rivard, B. S.; Münck, E.; Que, L., Jr.; Lipscomb, J. D. An Unusual Peroxo Intermediate of the Arylamine Oxygenase of the Chloramphenicol Biosynthetic Pathway. *J. Am. Chem. Soc.* **2015**, *137* (4), 1608–1617.
- (46) Knot, C. J.; Kovaleva, E. G.; Lipscomb, J. D. Crystal Structure of CmlI, the Arylamine Oxygenase from the Chloramphenicol Biosynthetic Pathway. *J. Biol. Inorg. Chem.* **2016**, *21* (5), 589–603.
- (47) Kulik, H. J.; Blasiak, L. C.; Marzari, N.; Drennan, C. L. First-Principles Study of Non-Heme Fe(II) Halogenase SyrB2 Reactivity. *J. Am. Chem. Soc.* **2009**, *131* (40), 14426.
- (48) Blanksby, S. J.; Ellison, G. B. Bond Dissociation Energies of Organic Molecules. *Acc. Chem. Res.* **2003**, *36* (4), 255–263.
- (49) Chiang, C.-Y.; Ohashi, M.; Le, J.; Chen, P.-P.; Zhou, Q.; Qu, S.; Bat-Erdene, U.; Hematian, S.; Rodriguez, J. A.; Houk, K. N.; Guo, Y.; Loo, J. A.; Tang, Y. Copper-Dependent Halogenase Catalyses Unactivated C–H Bond Functionalization. *Nature* **2025**, *638* (8049), 126–132.
- (50) Cutsail, G. E. I.; Banerjee, R.; Zhou, A.; Que, L., Jr.; Lipscomb, J. D.; DeBeer, S. High-Resolution Extended X-Ray Absorption Fine Structure Analysis Provides Evidence for a Longer Fe...Fe Distance in the Q Intermediate of Methane Monooxygenase. *J. Am. Chem. Soc.* **2018**, *140* (48), 16807–16820.
- (51) Papadopoulou, A.; Meierhofer, J.; Meyer, F.; Hayashi, T.; Schneider, S.; Sager, E.; Buller, R. Re-Programming and Optimization of a L-Proline Cis-4-Hydroxylase for the Cis-3-Halogenation of Its Native Substrate. *ChemCatChem* **2021**, *13* (18), 3914–3919.